methods

Coupled assay of sphingomyelin and ceramide molecular species by gas liquid chromatography

Claude Vieu,* François Tercé,* Françoise Chevy,† Corinne Rolland,* Ronald Barbaras,* Hugues Chap,* Claude Wolf,† Bertrand Perret,* and Xavier Collet[1],*

Institut Fédératif de Recherche Claude de Preval,* IFR 30, Institut National de la Santé et de la Recherche Médicale, Unité 326, Phospholipides membranaires, Signalisation cellulaire et Lipoprotéines, Hôpital Purpan, 31059, Toulouse Cedex, France; and Laboratoire Commun de Spectrométrie de masse,† Faculté de médecine de St Antoine, Université de Paris 6, Paris, France

Abstract **This study reports a single-step analysis of the molecular species of endogenous ceramides and of the ceramide moiety of sphingomyelins in biological samples, using gas liquid chromatography (GLC). Silylated sphingomyelins were quantitatively converted to monosilylated ceramide upon injection into GLC, whereas the free ceramides were di-silylated on the primary and secondary alcohol function, as confirmed by mass spectrometry. The reproducible shift of the retention times between the mono- and di-silylated derivatives enables simultaneous quantification of the variety of sphingomyelin and ceramide molecular species. Overlapping diacylglycerols were first removed by a mild alkaline treatment of the lipid extract. The lowest detection limit (5 pmol) did not allow for identification of free ceramides in human plasma, but 17 molecular species of ceramides derived from sphingomyelins were quantified, from NC16:0 up to NC24:1. By contrast, three major free ceramides (NC16:0, NC24:0, and NC24:1) were quantified in HEPG2 and Chinese hamster ovary (CHO) cells. Upon induction of apoptosis in CHO cells by C6-ceramide, we could follow the disappearance of the C6-ceramide, its partial conversion to C6-sphingomyelin, and the prominent increase of NC16:0 ceramide. Thus, our method represents a unique procedure of simultaneous analysis of sphingomyelin and ceramide molecular species able to monitor the variation of the different pools in biological samples.**—Vieu, C., F. Tercé, F. Chevy, C. Rolland, R. Barbaras, H. Chap, C. Wolf, B. Perret, and X. Collet. **Coupled assay of sphingomyelin and ceramide molecular species by gas liquid chromatography.** ***J. Lipid Res.*** **2002.** 43: **510–522.**

Supplementary key words mass spectrometry • apoptosis • lipid analysis • plasma • CHO cells • HepG2 cells

Sphingolipids are constituents of cellular membranes and of lipoproteins. The common backbone is the long chain amino base sphingosine (*trans*-4-sphingenine), and the ceramides refer to the *N*-acyl derivatives of sphingosine. For a decade now, ceramides have been widely studied as regulators of major cellular functions, i.e., apoptosis, proliferation, or senescence (1–5). Thus, in addition to the well known phosphatidylinositol and phosphatidylcholine cycles generating diacylglycerol as a lipid messenger, a sphingomyelin cycle has been defined, in which the accumulation of ceramide, as both a precursor for sphingomyelin synthesis and a product of its hydrolysis by neutral or acidic sphingomyelinases (6–8), leads to the activation of specific transduction pathways. In addition, short-chain permeable ceramides have also been shown to mimic the effects of natural ceramides (9). However, recent reports have questioned the real presence of ceramides in different examples of apoptosis induction (10, 11).

A variety of techniques have been previously used for the separation and analysis of ceramides, including thin layer chromatography, gas liquid chromatography (GLC), or HPLC (12–16) and, more recently, mass spectrometry (MS) (10, 17, 18). Molecular species of free ceramides, as regards the fatty acid composition, have been identified and quantitated in different cell types such as human platelets (18), erythrocytes (19), leukemia U937 cells (20), or skin fibroblasts (17). However, all the reported methods required either a multistep preparation of the lipid sample (e.g., pre-purification of the ceramide before anthroylation and HPLC) (20), or expensive mass spectrometry equipment (17). A comparative and recent review of the current methods emphasized the lack of a simple technique allowing the simultaneous measurement of sphingomyelin and ceramides in biological samples (21).

In the present study, we have used mild alkaline hydrolysis of ester lipids, as the only pre-treatment of total lipid

Abbreviations: BSTFA, (*N,O bis*) trimethylsilyl trifluoroacetamide; CE 17:0, cholesteryl heptadecanoate; CHO, Chinese hamster ovary; DG C14:0, dimyristoylglycerol; GLC, gas liquid chromatography; MS, mass spectrometry; MTBSTFA, *N*-methyl-*N*-(*tertio* butyl dimethylsilyl)-trifluoroacetamide; NC16:0 D18:1, ceramide with the palmitic acid C16:0, N linked to D-sphingosine; TG C51, triheptadecanoylglycerol; tBDMCS, *tertio* butyldimethylchlosilane; tBDMS, *tertio* butyl dimethylsilyl; TMCS, trimethylchlorosilane; TMS, trimethylsilyl.

[1] To whom correspondence should be addressed.
e-mail: collet@cict.fr

extract, taking advantage of the resistance of the fatty acid amide link of ceramides, and allowing removal of all overlapping diacylglycerols. Separation of silylated products was then achieved by GLC on the basis of their carbon numbers. Moreover, the thermal-cracking upon injection of silylated sphingomyelins into monosilylated ceramides enabled the separation of the molecular species of disilylated free ceramides from the monosilylated sphingomyelin-derived ceramides in a one-step chromatography. We have been able to determine the detailed composition of sphingomyelins and ceramides in plasma and in cultured cells, and to follow the metabolization of short chain ceramide after induction of apoptosis in Chinese hamster ovary (CHO) cells. The method provides a simple straightforward technique to assay the molecular species of ceramides derived from sphingomyelins and free ceramide interconversion in biological samples.

MATERIALS AND METHODS

Materials

(*N,O bis*) trimethylsilyl trifluoroacetamide (BSTFA) plus 1% trimethylchlorosilane (TMCS), *N*-methyl-*N*-(*tertio* butyl dimethylsilyl) trifluoroacetamide (MTBSTFA), and *tertio* butyl dimethylchlorosilane (tBDMCS) were obtained from Sigma (St. Quentin Fallavier, France). Dimethylformamide and acetonitrile were from Rathburn (Walker Burn, Scotland). Acetylchloride was from MERCK; chloroform, methyl alcohol, and ethylacetate (HPLC grade) were from CARLO ERBA, France. Stigmasterol, cholesteryl heptadecanoate, triheptadecanoylglycerol, 1,3 dimyristoylglycerol, *D*-sphingosine, triethylamine, tetrahydrofurane; pentadecanoyl- (C15:0), heptadecanoyl- (C17:0), arachidoyl- (20:0), behenoyl-(22:0)chloride; *N* palmitoyl *D*-sphingosine, *N* stearoyl *D*-sphingosine, *N* nervonoyl *D*-sphingosine, sphingomyelin from bovine brain, and sphingomyelinase from *Bacillus cereus* were from Sigma. C6-ceramide was from BIOMOL Research Labs (Plymouth Meeting, PA), and a stock solution was prepared at 50 mM in ethanol.

Ceramide synthesis

Four ceramides (C15:0-D18:1, C17:0-D18:1, C20:0-D18:1, and C22:0-D18:1) were generated according to Dijkman et al. (22). 40 μmol of *D*-sphingosine dissolved in 100 μl of water, and 20 μl of triethylamine was monoacylated by addition of 40 μmol of each acylchloride dissolved in 830 μl of tetrahydrofurane. The reaction mixture was stirred overnight at 37°C and evaporated to dryness with a vacuum pump. The residue was extracted (23), and the chloroform phase was filtered, evaporated to dryness, weighted, and finally dissolved in 7 ml of ethylacetate-methanol (1:1, v/v). A quantitative yield of 95% was obtained. An aliquot of each synthesized ceramide was silylated with BSTFA (1% TMCS)-acetonitrile(1:1, v/v), and the purity of the compounds was checked by GLC on a RESTEK 50 capillary column.

Chemical treatment of lipids

For the mild-acid treatment, four synthetic ceramides, NC15:0-D18:1, NC17:0-D18:1, NC20:0-D18:1, and NC22:0-D18:1 (10 μg each) were added to internal standards, stigmasterol (4 μg), 1-2 dimyristoylglycerol (6 μg), and cholesteryl heptadecanoate (6 μg). The mild acid treatment was performed by adding in a Teflon capped vial (8 ml), 1 ml of the fresh mixture of acetylchloride and water-free methanol (1:20, v/v), equivalent to a 3% solution of dry HCl in methanol, followed by 1 h incubation at 55°C on a heating sand bath as previously described (24). After evaporation of methanol and HCl under a stream of nitrogen, the samples were dissolved in 200 μl of silylation reagent, BSTFA (1% TMCS)-acetonitrile (1:1, v/v). Mild-acid treated ceramides were checked on the same RESTEK 50 capillary column.

For the mild-alkaline treatmentt, 1 ml of 0.6 *N* methanolic NaOH (containing 300 μl of water) was added to 0.5 ml methanol and 0.3 ml chloroform, and the total lipid extract dissolved in 200 μl ethyl acetate (0.3 *N* NaOH final concentration). After 10 min at 20°C, the solution was neutralized with 1.2 ml of 0.5 N methanolic HCl, 1.8 ml of water was added, and lipids were extracted with 2.1 ml of chloroform. After phase separation, the chloroform phase was filtered and evaporated to dryness, and lipids were resuspended with 200 μl ethylacetate.

Lipid extraction

Depending on the experiment, different internal standards were added before extraction. Total lipids were extracted (23) in 15 ml teflon-capped vials from biological samples recovered as follows: aliquots (40 μl) of human plasma were collected from normolipemic donors. Confluent HepG2 cells were washed three times in PBS, scrapped in NaCl 0.9%, and centrifuged; the pellet was resuspended in PBS and sonicated three times on ice for 30 s before extraction. For CHO cells experiments, at each incubation time cells were washed in PBS, scrapped in cold methanol-water (2:1, v/v), and sonicated for 10 s. An aliquot was retained for protein measurement before extraction.

Measurements of neutral lipid molecular species by GLC

Internal standards were added prior to lipid extraction: stigmasterol, *sn*-1-2 dimirystoyl glycerol (DG C14:0), cholesteryl heptadecanoate (CE C17:0), triheptadecanoyl glycerol (TG C51), and two synthetic ceramides (NC17:0-D18:1 and NC15:0-D18:1), to allow further quantification. The "mild-acid treatment" procedure (mild under anhydrous conditions) was applied to the synthetic ceramides used as standards in order to prepare quantitatively the dehydrated monosilylated forms, similar to those originating from sphingomyelins during the GLC separation. The chloroform phase was filtered, evaporated to dryness, and dissolved in 200 μl ethyl acetate. Lipids (1 μl injection) were analyzed on a non-polar capillary column (5 m × 0.31 mm i.d.) coated with cross-linked dimethyl siloxane (Ultra 1, Hewlett Packard) as described (25, 26). Oven temperature was programmed from 200°C to 335°C at a rate of 5°C/min with hydrogen as the carrier gas (0.5 bar). The response factors for lipid classes were determined from the internal standards.

Measurement of ceramides by GLC

The dry lipid extracts were dissolved in 200 μl of the silylation mixture, BSTFA (1% TMCS)-acetonitrile (1:1, v/v) overnight at 20°C plus 30 min at 40°C, and analyzed by GLC on a capillary column (30 m × 0.32 mm i.d.) coated with phenyl (50%), methyl (50%) siloxane (Restek 50). Oven temperature was programmed from 210°C to 330°C at the rate of 4°C/min, with hydrogen as the carrier gas (1 bar). Trimethylsilyl (TMS) ether-ceramide molecular species were resolved on the basis of their carbon number and the unsaturation of fatty acids and *D*-sphingosine (12, 27). The response factors for lipid species were determined from the internal standards.

Mass spectrometry

The TMS derivatives of ceramides were analyzed by gas liquid chromatography (Hewlett Packard 5890) coupled with mass spectrometry (Nermag, R10-10C, France). The GLC step on a nonpolar capillary column of cross-linked dimethyl silicone (19 m × 0.31 mm i.d.) (ULTRA1 Agilent Technologies, France) achieved

the separation of the ceramide derivatives on the basis of their acyl chain length (12) in the temperature range from 245°C to 345°C, scanned at the rate of 6°C/min. The ceramides were also treated with the silylation reagent, MTBSTFA (100 μl) in acetonitrile (80 μl) and dimethylformide (20 μl) containing *tertio* butyl dimethylsilyl (tBDMS) (5%), which form tBDMS derivatives. The sample was introduced in the splitless mode with the injector temperature set at 345°C. The mass spectrometer interface was heated at 345°C and the ionization source at 200°C. The ceramide derivatives were identified by the positive fragment ions

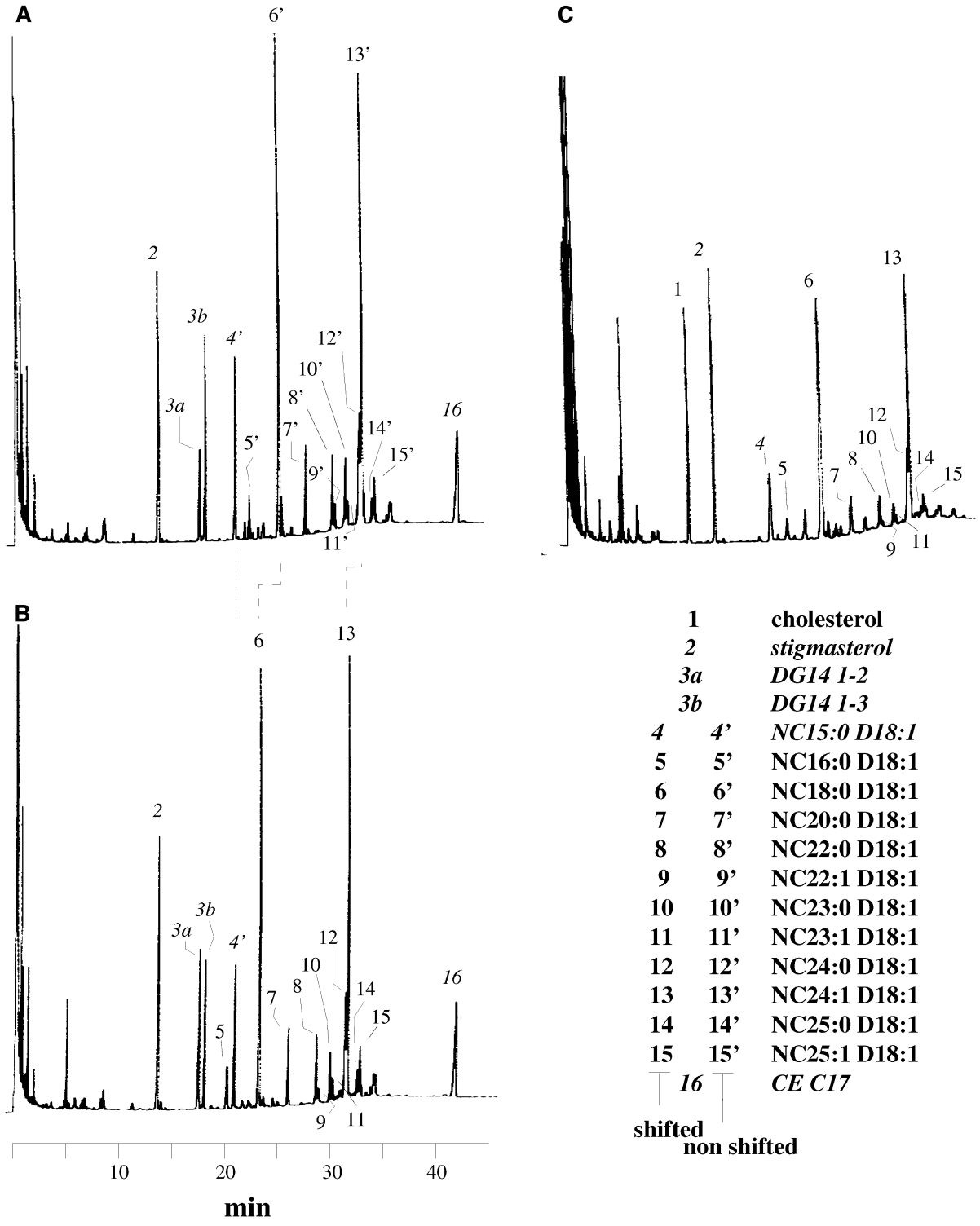

Fig. 1. Gas liquid chromatogram of bovine brain sphingomyelins and ceramides. Sphingomyelins from bovine brain were either treated with sphingomyelinase (2.5 units during 2 h) (A and C) or untreated (B), without (A and B), or followed by (C) mild-acid treatment. The samples were then converted to trimethylsilyl (TMS) ether derivatives and the ceramide profile was analyzed on a RESTEK 50 capillary column as described in Materials and Methods. Before lipid extraction, four internal standards (in italic) were added: stigmasterol (4 μg), *sn*-1-2 dimyristoyl glycerol (6 μg), cholesteryl heptadecanoate (6 μg), and ceramide with the palmitic acid (NC15:0-D18:1) (6 μg).

and the quasi-molecular ion (adduct $M+H^+$) produced in the chemical ionization mode by ammonia (0.1 bar). The mass scanning of the quadrupole (2.2 s/scan) was set from *m/z* 50 to 850, or 990 for TMS or tBDMS derivatives, respectively. TBDMS has been used for some MS experiments because it gives a very prominent M-57 ion easily identified.

Cell culture

The human hepatoblastoma-derived cell line HepG2 was cultured as described (28). Cells were plated at 2×10^6 cells per flask (T75 cm^2) and grown in DMEM supplemented with 10% FBS, 100 U/ml penicillin, and 100 μg/ml streptomycin at 37°C in a 5% CO_2 and 95% air incubator. Medium was changed every 2 or 3 days, and the cells were sub-cultured every 6 days. CHO K1 cells were grown in Ham's F-12 medium, supplemented with bovine pancreatic insulin (20 μg/ml) and 10% FBS in the presence of penicillin and streptomycin, as described (29). For the experiments with NC6:0 D18:1 (C6-ceramide), CHO cells were seeded at 10^6 cells in 100 mm Petri dishes and incubated 36 h before addition of C6-ceramide (50 μM final concentration).

Cell proliferation and apoptosis measurements

CHO cells were treated with C6-ceramide as described above. At each time point, medium containing floating cells was discarded; and cells on the plate were washed in PBS, gently scrapped in PBS-EDTA 1 mM, washed again in PBS, and counted on a coulter Z1 (Beckman-Coulter). Cells were fixed in 70% ice-cold ethanol and kept at −20°C until analysis. Following propidium iodide labeling, apoptosis was measured by fluorescence analysis cell sorter (29).

Analytical procedures

Proteins were measured according to Lowry et al. (30). Total and unesterified cholesterol were determined enzymatically (31) using commercial kits (Boehringer, Mannheim, F. R. G.). Phospholipids were estimated as the lipid phosphorus, according to Böttcher et al. (32).

RESULTS

Identification of ceramide molecular species produced from bovine brain sphingomyelin after sphingomyelinase treatment or mild-acid treatment

We previously described a GLC method to identify the silylated diacylglycerol molecular species in biological samples with a separation based on the carbon number and the double bond content of fatty acids (26). In order to develop a similar method for the identification of the ceramide molecular species, a sample of bovine brain sphingomyelin was treated by sphingomyelinase. The ceramides thus produced were analyzed by GLC, after silylation in the form of TMS-derivatives, and were quantified in the presence of internal standards (stigmasterol, dimyristoyl glycerol, cholesteryl heptadecanoate, and the ceramide NC15:0-D18:1) prepared according to Materials and Methods (**Fig. 1A**). Eleven distinct molecular species of ceramides were resolved and the putative structures were assessed by comparison with the retention times of the silylated reference standards, including four ceramides (NC15:0-, NC17:0-, NC20:0-, and NC22:0-D18:1) prepared according to Materials and Methods and three commercially available ceramides (NC16:0-, NC18:0-, and NC24:1-D18:1). The molecular species were baseline-separated according to their

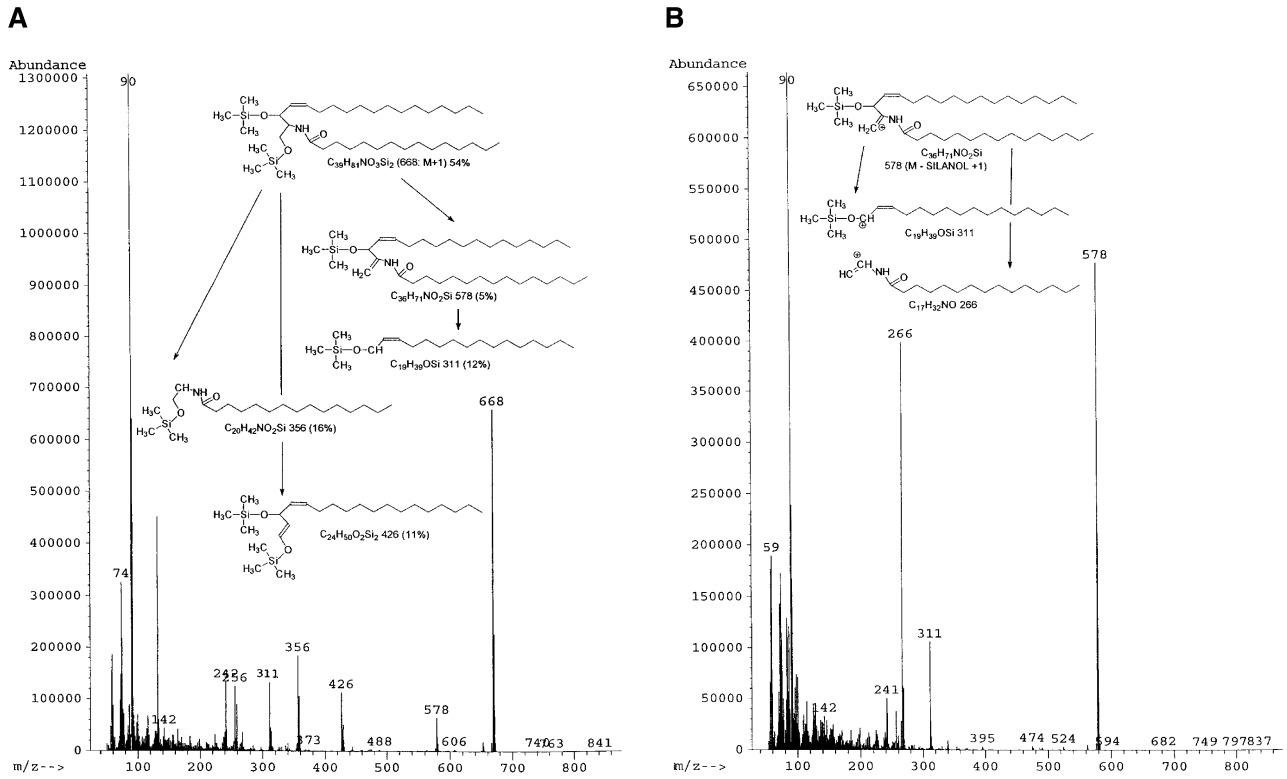

Fig. 2. Mass spectrum profiles of ceramide with the palmitic acid (NC15:0-D18:1) [trimethylsilyl (TMS) derivatives and chemical ionization by ammonia]. Mass spectrometric data for TMS derivatives of NC15:0-D18:1 1 before (A) and after (B) mild-acid treatment treatment, performed as described in Materials and Methods.

carbon number and degree of unsaturation as previously described by Kuksis and colleagues (12, 27). Thus, NC24:1-D18:1 (Fig. 1A, peak 13′) was eluted after NC24:0-D18:1 (Fig. 1A, peak 12′). NC24:1-D18:1 and NC18:0-D18:1 were found to be the major components of the bovine brain sphingomyelins (35.6% and 31.7%, respectively).

In a separate experiment, sphingomyelinase-untreated samples were analyzed under the same derivatization and GC conditions (Fig. 1B). The peaks of the four internal standards (stigmasterol, DG C14, NC15:0-D18:1, and CE C17) had the same retention times, but surprisingly, a profile of ceramide molecular species appeared, similar to the profile obtained with the sphingomyelinase-treated sphingomyelins. In addition, the "ceramide-like" profile was shifted to a retention time shorter by about 2 min, as compared with the original ceramide profile. For example, NC16:0-D18:1 (Fig. 1B, peak 5) was then eluted before the internal standard NC15:0-D18:1 (Fig. 1A, peak 4′). It is noteworthy that a similar quantitative yield of ceramide molecular species was obtained from sphingomyelinase-treated or -untreated samples.

As the diacylglycerols and ceramide molecular species overlapped in the chromatogram (12), the samples of Fig. 1A were treated under acidic conditions (mild-acid treatment which selectively cleaved ester bonds of neutral lipids and phospholipids), before silylation (Fig. 1C). Interestingly, sphingomyelinase-treated samples (Fig. 1C) and untreated samples (not shown) gave an identical profile. As expected, DG C14:0 and CE C17:0 were absent and a peak of free cholesterol (peak 1) appeared, confirming the fatty acyl cleavage of neutral lipids. Moreover, the profiles were similar to Fig. 1B (shifted peaks), except that the internal standard NC15:0-D18:1 was also shifted to 2 min earlier. Interestingly, the mild-acid treatment also induced a partial ceramide hydrolysis (cleavage of the amide bond), with a recovery of only 50% (compare for instance the NC18:0-D18:1 between peak 6 in Fig. 1C and peak 6′ or 6 in Fig. 1A and B). However, the remaining ceramides were completely converted to the unique molecular species with a lower retention time, suggesting a lower molecular mass. Thus, injection of either directly silylated or mild-acid-treated and then silylated sphingomyelins, generated ceramide molecular species displaying the same reproducible shift, i.e., a lower retention time.

In order to explain the chemical alterations underlying the GLC shift, we achieved a comparative GC-MS analysis of ceramide before and after the mild acid treatment (**Fig. 2A** and **B**). The mass spectrum of silylated NC15:0 D18:1 indicated a prominent quasi-molecular ion at *m/z*

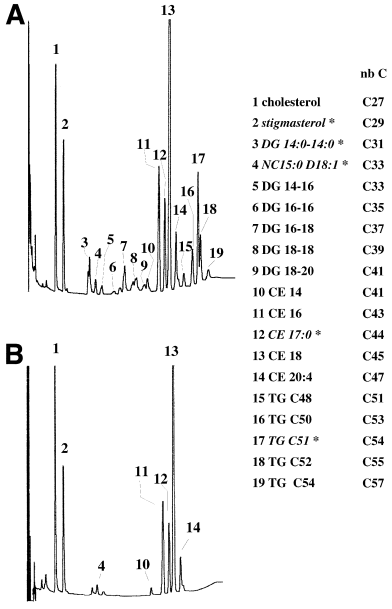

Fig. 3. Gas liquid chromatogram of the neutral lipid molecular species of plasma (40 μl) before (A) and after (B) mild alkaline treatment of lipids. Analysis of total lipid extract was performed on an Ultra 1 Hewlett Packard fused silica capillary column coated with cross-linked methyl silicone as described in Materials and Methods. Free cholesterol, diacylglycerols, cholesteryl esters, and triacylglycerols molecular species were determined based on total carbon number. B: The profile of neutral lipids after a mild alkaline treatment of the lipid extract. Before lipid extraction, five internal standards (*, in italic) were added: stigmasterol (4 μg), *sn*1-2 dimyristoyl glycerol (6 μg), cholesteryl heptadecanoate (6 μg), triheptadecanoylglycerol (6 μg), and NC15:0-D18:1 (6 μg).

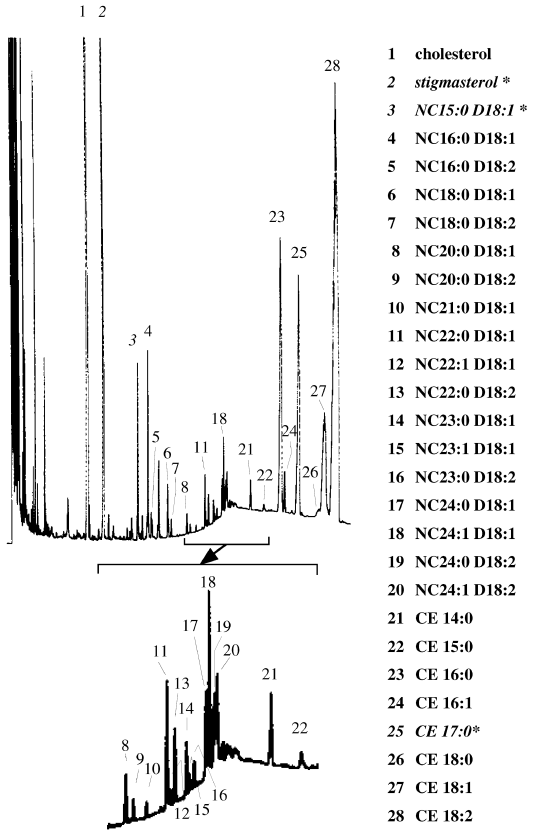

Fig. 4. Gas liquid chromatogram of sphingomyelin-derived ceramide molecular species from plasma. Total lipids extract from plasma (40 μl) was submitted to mild alkaline hydrolysis and converted to trimethy silyl ether derivatives. Gas liquid chromatography was performed on a RESTEK 50 capillary column as described in Materials and Methods. * Internal standards were as in Fig. 1. Peaks 8–22 were magnified.

668 (M+1) which was consistent with a di-TMS derivative. The occurrence of both fragment ions at *m/z* 426 and 311 confirmed the derivatization of the alcohol at positions 3 and 1 (insert in Fig. 2A shows the ion abundance). In contrast after the mild acid treatment under strictly anhydrous conditions, the spectrum was consistent with dehydration of the primary alcohol at position 1, and the derivatization of the secondary alcohol left at position 3 as indicated by the abundant positive ions at *m/z* 578 for NC15 D18:1 (M+1). The α-cleavage initiated by the radical site created on the amide nitrogen and the ether oxygen induced the fragment ions 311 and 266 after cleavage of *D*-sphingosine between C2 and C3 (insert in Fig. 2 shows the ion abundance).

The mass spectra of the tBDMS derivatives showed a prominent M-57 ion corresponding to the cleavage of the *tertio* butyl moiety. In the chemical ionization mode, the quasi-molecular ions M-57+H^+ (at *m/z* 709, 737, 764, and 792) appeared for the disilylated derivatives of NC16:0-, NC18:0-, NC20:0-, and NC22:0-D18:1 ceramides, respectively. After the application of mild acid under anhydrous conditions, the abundant quasi-molecular ion pointed to a dehydrated mono-silylated derivative of the ceramide, M-18+H^+ (at *m/z* 634, 662, 690, and 718 for NC16:0-, NC18:0-, NC20:0-, and NC22:0-D18:1 ceramides, respectively), and M-18-57 fragment ions (at *m/z* 576, 604, 632, and 660) (not shown). Although tBDMS derivation was useful for MS analysis, the NC24:1-D18:2 derivative overlapped with CE C14:0 on a Restek 50 column. For this reason, further experiments were conducted with TMS derivatives.

Therefore, mass spectrometry confirmed that the shift of GLC retention times represented the separation of disilylated ceramides at positions 1 and 3, originating from the ceramide alcohol group present, whereas monosilylated derivative at position 3 originated from cleavage of the phosphorylcholine group followed by dehydration. Whether the ceramide-like monosilylated derivatives originated from the sphingomyelins in the heated injector port of GLC or from chemical alterations, the structures were found identical on the basis of mass spectrometry (not shown). A useful result for further application in biology is that the monosilylated ceramides were formed from the sphingomyelin species after the complete thermal cracking in the GLC injector heated to 305°C. Starting from this result, a single-step GLC separation of ceramides and precursor sphingomyelins became available.

In order to assess the accuracy of the method, we have performed calibration curves. We have submitted stan-

TABLE 1. Identification of TMS-ceramides derived from sphingomyelins in human plasma

	MW of Ceramide Moiety	Relative Retention Time	nmol/ml	mol (%)
Cholesterol	386.6	11.71 ± 0.12	1,403.0 ± 137.1	
Stigmasterol[a]	*412.7*	*13.97 ± 0.11*		
SM molecular species				
NC15:0-D18:1[a]	*523.8*	*18.91 ± 0.06*		
NC16:0-D18:1	537.9	20.41 ± 0.04	195.5 ± 50.5	37.34 ± 1.43
NC16:0-D18:2	535.9	21.01 ± 0.04	16.0 ± 0.6	3.22 ± 0.69
NC18:0-D18:1	566.0	23.30 ± 0.04	49.3 ± 13.4	9.41 ±0.86
NC18:0-D18:2	564.0	23.79 ± 0.05	10.8 ± 4.2	2.02 ± 0.51
NC20:0-D18:1	594.0	26.04 ± 0.05	19.8 ± 6.5	3.73 ± 0.39
NC20:0-D18:2	592.0	26.52 ± 0.06	5.5 ± 1.7	1.04 ± 0.19
NC21:0-D18:1	608.0	27.37 ± 0.06	6.6 ± 2.6	1.23 ± 0.22
NC22:0-D18:1	622.0	28.64 ± 0.07	39.2 ± 13.7	7.29 ± 0.74
NC22:1-D18:1	620.0	28.84 ± 0.06	7.9 ± 1.8	1.55 ± 0.27
NC22:0-D18:2	620.0	29.14 ± 0.07	18.9 ± 8.9	3.4 ± 0.87
NC23:0-D18:1	636.0	29.91 ± 0.06	15.3 ± 5.5	2.85 ± 0.27
NC23:1-D18:1	634.0	30.09 ± 0.06	7.9 ± 2.1	1.56 ± 0.38
NC23:0-D18:2	634.0	30.40 ± 0.08	6.9 ± 2.6	1.27 ± 0.17
NC24:0-D18:1	650.1	31.15 ± 0.07	25.0 ± 8.0	4.69 ± 0.42
NC24:1-D18:1	648.1	31.34 ± 0.07	57.3 ± 8.3	11.24 ± 1.39
NC24:0-D18:2	648.1	31.67 ± 0.08	19.5 ± 6.7	3.64 ± 0.58
NC24:1-D18:2	646.1	31.86 ± 0.08	23.9 ± 6.9	4.52 ± 0.47
Total			525.6 ± 139	100
Cholesteryl ester				
CE14:0	597.0	35.30 ± 0.09	35.0 ± 9.3	1.00 ± 0.26
CE15:0	611.0	37.23 ± 0.09	7.2 ± 1.8	0.20 ± 0.05
CE16:0	625.1	39.66 ± 0.11	474.0 ± 51.2	13.53 ± 1.63
CE16:1	623.1	40.25 ± 0.13	109.8 ± 82.8	3.18 ± 2.36
CE17:0[a]	*639.1*	*42.29 ± 0.10*		
CE18:0	653.1	45.28 ± 0.16	23.87 ± 3.51	16.88 ± 1.32
CE18:1	651.1	46.07 ± 0.14	554.0 ± 77.5	16.15 ± 4.20
CE18:2	649.1	47.85 ± 0.18	1,759.3 ± 426.8	49.05 ± 6.65
Total			3,536.1 ± 429.1	100

Total lipid extracts were derivatized and sphingomyelin molecular species were identified on the basis of the ceramide moiety analysis by gas liquid chromatography as in Fig. 4. Each molecular species was numbered based upon its retention time. (a and italic): standards. Cholesteryl esters molecular species were also quantitated.

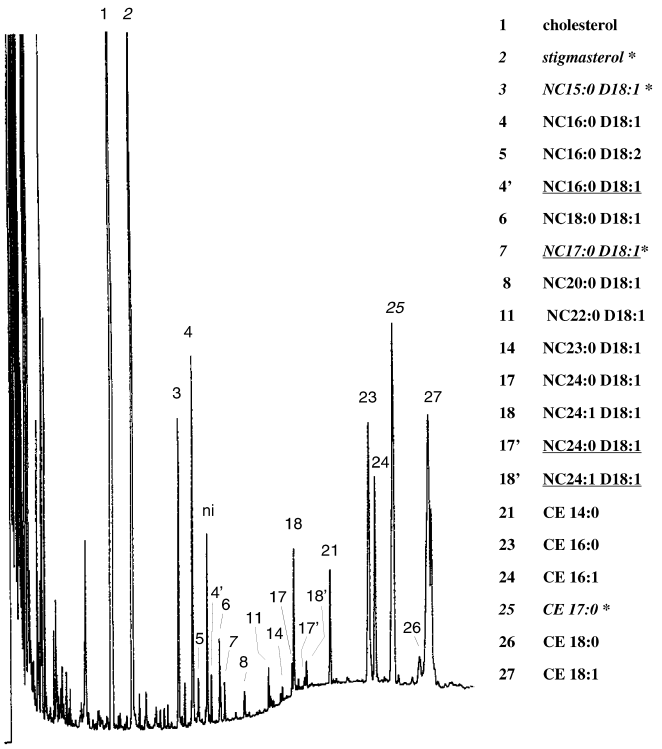

Fig. 5. A typical profile of free and sphingomyelin-derived ceramide molecular species in HepG2 cells. Lipids were extracted from HepG2 cells (1 mg prot.), and treated and analyzed as in Fig. 4 and Materials and Methods. The disilylated forms of ceramides were underlined. * Internal standards were as in Fig. 1.

dards of mono- or disilylated ceramides to the multiple steps (extraction, base hydrolysis, derivatization, and injection port vaporization). The results indicated that the different mono- or disilylated ceramides have the same behavior (not shown). In addition, these curves allow to define the threshold of detection around 5 pmol.

Identification of ceramide and sphingomyelin molecular species in biological samples after mild alkaline treatment

In order to avoid the cleavage of sphingomyelins and the hydrolysis of ceramides, as induced by the acid anhydrous treatment (Fig. 1C), we then used a mild-alkaline hydrolysis to remove the overlapping diacylglycerols. A typical profile of neutral lipid molecular species in plasma was obtained by GLC according to the total carbon number (Cn) on the non-polar Ultra1 column (**Fig. 3A**). Four internal standards allowed us to quantify unesterified and esterified cholesterol, diacylglycerols, and triacylglycerols. After mild alkaline treatment of the lipid extract, the profile of neutral lipids showed a complete hydrolysis of diacylglycerols and triacylglycerols (Fig. 3B). NC15:0 D18:1 was not susceptible to such a treatment. Under the mild conditions used throughout the study, cholesteryl esters were mostly resistant (however, up to 15% hydrolysis could occur). To allow a base-line resolution of the sample, further analyses were performed on the medium polar column (Restek 50) after silylation of alkaline treated extracts.

Three biological samples were analyzed: human plasma,

TABLE 2. Identification of TMS-ceramides isolated from HepG2

	MW of Ceramide Moiety	Relative Retention Time	nmol/mg prot (n = 4)		mol (%)	
			SM	Ceramide	SM	Ceramide
Cholesterol	386.6	11.73 ± 0.03	77.62 ± 7.60			
Stigmasterol[a]	*412.7*	*13.94 ± 0.03*				
SM/ceramide						
NC15:0-D18:1[a]	*523.8*	*18.84 ± 0.04*				
NC16:0-D18:1	537.9	20.34 ± 0.04	12.34 ± 0.62		55.24	
NC16:0-D18:2	535.9	20.93 ± 0.04	1.59 ± 0.57		7.12	
NC16:0-D18:1	**537.9**	**22.32 ± 0.04**		**2.00 ± 0.33**		**63.31**
NC18:0-D18:1	566.0	23.20 ± 0.04	2.31 ± 0.07		10.34	
NC17:0-D18:1[a]	*580.0*	*23.69 ± 0.03*				
NC20:0-D18:1	594.0	25.92 ± 0.04	0.83 ± 0.03		3.72	
NC22:0-D18:1	622.0	28.52 ± 0.05	1.26 ± 0.27		5.64	
NC23:0-D18:1	636.0	29.97 ± 0.06	0.48 ± 0.09		2.15	
NC24:0-D18:1	650.1	31.00 ± 0.04	0.68 ± 0.04		3.04	
NC24:1-D18:1	648.1	31.21 ± 0.04	2.85 ± 0.45		12.76	
NC24:0-D18:1	**650.1**	**32.37 ± 0.04**		**0.44 ± 0.08**		**13.71**
NC24:1-D18:1	**648.1**	**32.46 ± 0.07**		**0.77 ± 0.06**		**23.99**
Total			22.3 ± 2.14	**3.21 ± 0.47**	100	**100**
Cholesteryl ester						
CE14:0	597.0	35.19 ± 0.07	3.92 ± 2.06		6.99	
CE15:0						
CE16:0	625.1	39.49 ± 0.12	14.22 ± 7.9		25.35	
CE16:1	623.1	40.14 ± 0.08	7.47 ± 2.61		13.32	
CE17:0[a]	*639.1*	*42.08 ± 0.10*				
CE18:0	653.1	45.00 ± 0.15	2.68 ± 2.01		4.78	
CE18:1	651.1	45.95 ± 0.16	27.81 ± 6.39		49.57	
Total			56.1 ± 24.8		100	

Free (bold) or sphingomyelin derived ceramides were extracted, derivatized, and identified by gas liquid chromatography as in Fig. 5. Each molecular species was numbered based upon its retention time. (a and italic): standards. Cholesteryl ester molecular species were also quantified.

TABLE 3. Identification of TMS-ceramides isolated from CHO cells

	MW of Ceramide Moiety	Relative Retention Time	nmol/mg prot (n = 6)		mol (%)	
			SM	Ceramide	SM	Ceramide
Cholesterol	386.6	11.73 ± 0.03	196.2 ± 55.9			
Stigmasterol[a]	*412.7*	*13.94 ± 0.03*				
SM/ceramide						
NC15:0-D18:1[a]	*523.8*	*18.84 ± 0.04*				
NC16:0-D18:1	537.9	20.34 ± 0.04	54.94 ± 10.65		77.30	
NC16:0-D18:2	535.9	20.93 ± 0.04	6.74 ± 2.35		9.12	
NC16:0-D18:1	537.9	22.32 ± 0.04		**1.85 ± 0.41**		**74.00**
NC18:0-D18:1	566.0	23.20 ± 0.04	4.29 ± 0.91		5.80	
NC22:0-D18:1	622.0	28.52 ± 0.05	1.10 ± 0.21		1.49	
NC23:0-D18:1	636.0	29.97 ± 0.06	0.27 ± 0.03		0.37	
NC24:0-D18:1	650.1	31.00 ± 0.04	1.85 ± 0.47		2.50	
NC24:1-D18:1	648.1	31.21 ± 0.04	4.75 ± 0.98		6.42	
NC24:0-D18:1	650.1	32.37 ± 0.04		**0.29**		**11.60**
NC24:1-D18:1	648.1	32.46 ± 0.07		**0.36**		**14.40**
Total			74.78 ± 12.62	**1.96 ± 0.24**	100	**100**
Cholesteryl ester						
CE14:0	597.0	35.19 ± 0.07	12.65 ± 5.88		13.90	
CE15:0			0.92 ± 0.51		1.01	
CE16:0	625.1	39.49 ± 0.12	23.50 ± 13.05		25.82	
CE16:1	623.1	40.14 ± 0.08	6.67 ± 3.05		7.33	
CE17:0[a]	*639.1*	*42.08 ± 0.10*				
CE18:0	653.1	45.00 ± 0.15	4.51 ± 3.79		4.95	
CE18:1	651.1	45.95 ± 0.16	42.77 ± 19.41		47.00	
Total			91.01 ± 44.86		100	

Free (bold) or sphingomyelin derived ceramides were extracted, derivatized, and identified by gas liquid chromatography for CHO cells. Each molecular species was numbered based upon its retention time. (a and italic): standards. Cholesteryl ester molecular species were also quantified.

human hepatoma cells (HepG2), and CHO cells, to assess the usefulness of the method. When lipid extracts from plasma sample were injected (**Fig. 4**), only shifted dehydrated peaks appeared, indicating sphingomyelin origin. The retention time and the quantitation of the different molecular species of sphingomyelins are presented in the **Table 1**. We identified 17 molecular species of sphingomyelins using mild-acid-treated NC15:0-D18:1 as an internal standard. The NC16:0-D18:1, NC24:1-D18:1, NC18:0-D18:1, and NC22:0-D18:1 represented the four major molecular species (37.3%, 11.2%, 9.4%, and 7.3%, respectively) as previously described (27). Identification of the minor 18:2 backbone has been done by reference to previous publications (12, 13, 27). In these conditions, natural ceramides (non-shifted peaks) were not detectable in plasma.

Analysis of cellular lipid extract from HepG2 cells (**Fig. 5**) showed both shifted and non-shifted peaks, representative of ceramides generated from sphingomyelins and endogenous ceramides, respectively. In this experiment, a synthetic non-mild-acid treated standard (NC17:0-D18:1) was used to quantify the natural ceramide molecular species. The three major molecular species of ceramides (monosilylated) generated from sphingomyelins corresponded to NC16:0-D18:1, NC24:1-D18:1, and NC18:0-D18:1 (55.2%, 12.8%, and 10.3%, respectively). In contrast to plasma, we were able to identify three molecular species of disilylated (natural) ceramides present in HepG2 cells, the NC16:0-D18:1, and NC24:1-D18:1, and NC24:0-D18:1 (63%, 24%, and 13%, respectively). The different compositions are given in **Table 2** with retention times and relative amount expressed as nmol/mg protein.

Analysis of CHO cell ceramide molecular species allowed the identification of seven molecular species of monosilylated ceramides generated from sphingomyelins (**Table 3**). The four major species corresponded to NC16:0-D18:1, NC16:0-D18:2, NC24:1-D18:1, NC18:0-D18:1, and (77.3%, 9.1%, 6.4%, and 5.8% respectively). The three molecular species of disilylated ceramides present in CHO cells were similar to HepG2 [NC16:1-D18:1 (74%), NC24:1-D18:1 (14%), and NC24:0-D18:1 (12%)]. In addition to ceramide analysis, our method allowed us to identify and to quantify the cholesteryl ester molecular species in the different lipid extracts (Figs. 4 and 5, and Tables 1–3).

Analysis of ceramides formed in CHO cells after treatment by sphingomyelinase or apoptosis induced by C6-permeant ceramide

In order to illustrate the usefulness of the method, an experiment was designed that monitored the balance between the ceramide formation and the degradation of sphingomyelins as induced by bacterial sphingomyelinase treatment of CHO cells (**Fig. 6**). It clearly appeared that the disappearance of the two major molecular species of sphingomyelins, (C16 and C24, as measured by the monosilylated forms) as a function of time of treatment, paralleled the appearance of the disilylated forms of ceramides.

Apoptosis is a physiological situation often associated with (triggered and/or followed by) the production of endogenous ceramides. The GLC method was applied to fol-

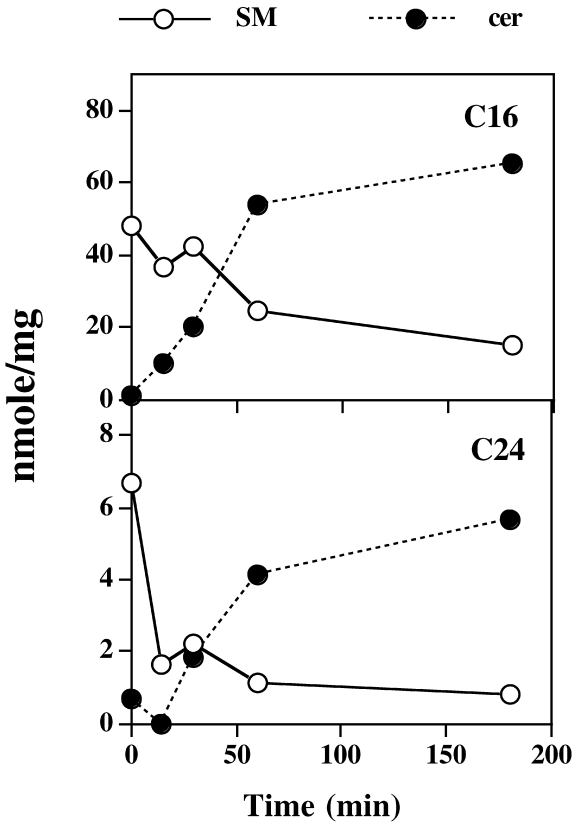

Fig. 6. Kinetics of the major ceramide formation after sphingomyelinase treatment of Chinese hamster ovary (CHO) cells. CHO cells (3×10^6) were treated by sphingomyelinase (30 mU/ml). Lipids were extracted, treated, and analyzed as in Fig. 4. Free (closed circle) or sphingomyelin-derived (open circle) major molecular species of ceramides (NC16:0-D18:1 and NC24:0-D18:1 + NC24:1-D18:1) were plotted as a function of incubation time.

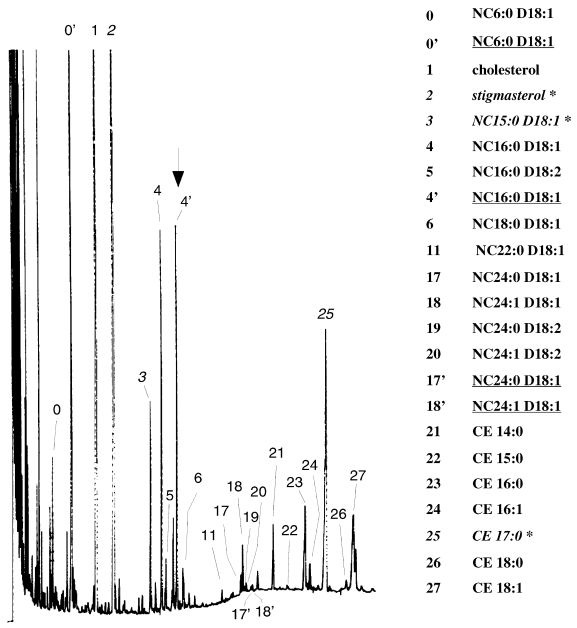

Fig. 7. A typical profile of free and sphingomyelin-derived ceramide molecular species in CHO cells after C6 ceramide treatment. CHO cells were treated with 50 μM of C6 ceramide for 2 h. Lipids were extracted and analyzed as in Fig. 4 and Materials and Methods. The disilylated forms of ceramides were underlined. * Internal standards were as in Fig. 1. The arrow indicated the appearance of the unshifted NC16:0-D18:1 (peak 4′).

low the sphingomyelin/ceramide balance, when apoptosis was induced by the addition of a short chain permeant ceramide to CHO cells. A typical profile after 2 h incubation with NC6:0-D18:1 indicated the presence of a major peak of disilylated NC6:0-D18:1 ceramide (peak 0′), reflecting the uptake of the permeant compound by the cells (**Fig. 7**). Furthermore, the mono-silylated "shifted" analog (peak 0) was also detected, indicating the conversion of the short chain ceramide into a short chain sphingomyelin, which was cracked upon GLC injection. In addition, a huge increase of the disilylated NC16:0-D18:1 (peak 4′) was observed, associated with a small increase of the monosilylated counterpart (peak 4), when compared with control cells (Table 3).

A typical time course experiment for 24 h indicated that the addition of NC6:0-D18:1 induced a rapid decrease in the cell number associated with apoptotic cells detected after 15 h (**Fig. 8A**). As shown above, a dramatic and rapid increase of the long-chain disilylated NC16:0-D18:1 ceramide was observed during the first 2 h (53.2-fold) and maintained up to 24 h (Fig. 8B), whereas NC24:0-D18:1 only slightly increased (2.25-fold) (Fig. 8C). This indicated a clear specificity toward disilylated NC16:0-D18:1 formation upon short chain ceramide treatment. In contrast with the former experiment with the sphingomyelinase (Fig. 6), monosilylated NC16:0-D18:1 and NC24:0-D18:1 slightly increase (by 1.65- and 2-fold respectively at 2 h, before returning back to the basal level), indicating the absence of sphingomyelin degradation. Finally, we were also able to analyze the uptake of disilylated NC6:0-D18:1 in the first 2 h followed by its conversion (Fig. 8D) into monosilylated NC6:0, demonstrating the conversion of the C6 ceramide into C6 sphingomyelin.

We confirmed the identification of the chemical structure of ceramides present in cellular extracts by GC-MS analysis after 2 h of incubation with C6:0 ceramide. Identification of both NC6:0-D18:1 taken up in CHO cells and the appearance of the major species detected NC16:0-D18:1 confirmed the presence of both mono- (sphingomyelin derived) and di-silylated (ceramide derived) forms by the major ions at *m/z* 452 and 542 (NC6:0-D18:1 sphingomyelin and ceramide derived) and 592, 682 (NC16:0-D18:1), respectively (not shown).

DISCUSSION

We report a simple and rapid method for the simultaneous assay of ceramides and sphingomyelins with molecular species resolution in biological samples. The development was based on an original observation that the silylated sphingomyelins are specifically converted to monosilylated ceramides upon injection into GLC, whereas silylated ceramides remain disilylated (Fig. 1A and B). Mono and disily-

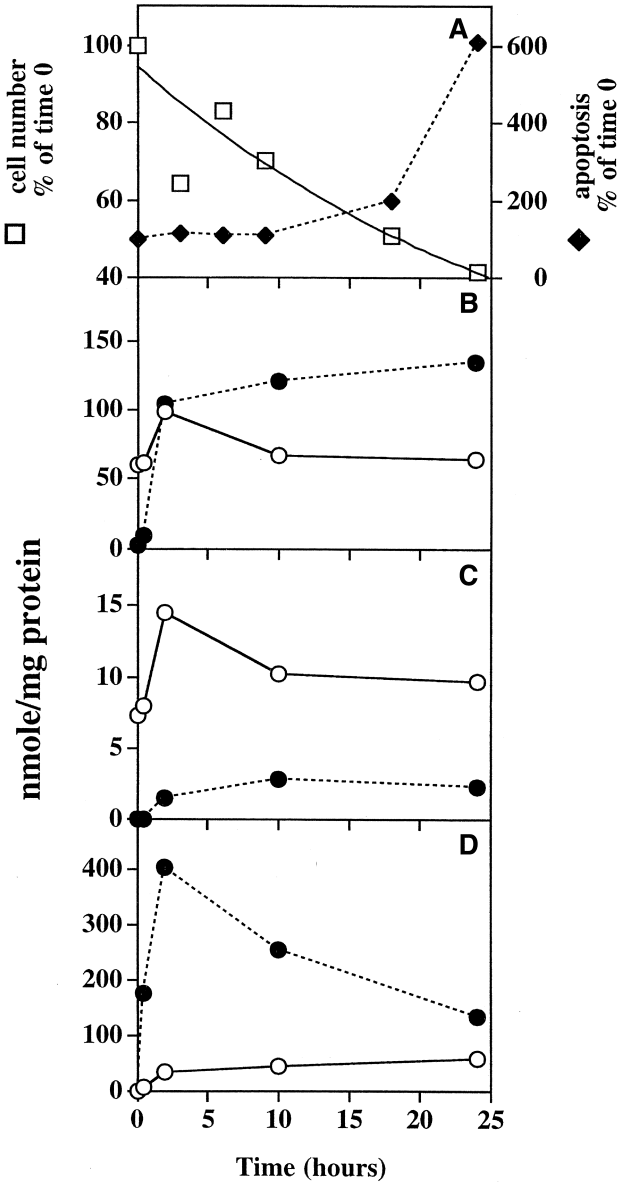

Fig. 8. Effect of C6 ceramide on apoptosis induction and ceramide metabolism in CHO cells. CHO cells were treated as in Fig. 7. At each incubation time, cell growth and apoptosis (A) were analyzed as described in Materials and Methods. Lipids were extracted and analyzed as in Fig. 4. Free (closed circle) or sphingomyelin-derived (open circle) molecular species of ceramides NC16:0-D18:1 (B), NC24:0-D18:1 + NC24:1-D18:1 (C), and NC6:0-D18:1 (D) were plotted as a function of incubation time. One experiment representative of three independent experiments.

lated ceramide structure was assigned by mass spectrometry (Fig. 2A and B). Taking advantage of the very reproducible difference in the retention times (2 min) between the mono- and disilylated forms, the simultaneous identification of sphingomyelin and ceramide molecular species can be achieved.

The cleavage of silylated sphingomyelins in the Ros injector is the consequence of temperature cracking which follows the evaporation of the solvent on the glass needle heated at 305°C. Under hydrogen, the specific cleavage of sphingomyelins into monosilylated ceramides releases the phosphorylcholine moiety (**Fig. 9**). The phosphoric acid residue has already been described to act as a dehydration catalyst for glycerophospholipids heated under the ammonia reagent gas, used for the purpose of direct chemical ionization mass spectrometry (33). Indeed, when the acidic function of bovine brain sphingomyelin was methylated by diazomethane, the formation of monosilylated ceramides was inhibited by 70% (not shown), which favors the actual role of the phosphoric acid group in the temperature-induced cracking.

Furthermore, the mild acid anhydrous condition of the mild-acid treatment procedure induces the same transformation, in addition to the partial cleavage of the amide bond. Indeed, the remaining silylated sphingomyelins are also temperature cracked and became identical to the ceramides dehydrated by the acid anhydrous conditions, both generating monosilylated ceramides (Fig. 9). The primary alcohol group of ceramide at position 1 is completely converted to the alkene bond between C1 and C2 after 1 h at 55°C, as confirmed by mass spectrometry (Fig. 2). A mechanism has been proposed that involved the protonated form of the primary alcohol, which dissociates into a carbonium ion and water. Secondarily the carbonium ion looses a hydrogen ion and the alkene is formed. Thus, the reactions of thermal-cracking or mild-acid treatment allow the formation of the similar 2-alkene bond of the monosilylated form of ceramide. We took advantage of the acid induced dehydration reaction to produce the monosilylated ceramide standard (NC15:0 D18:1) in order to quantify sphingomyelin molecular species. We can also rule out that some monosilylated ceramide could come from the thermal cracking of disilylated ceramide as standard NC15 (Fig. 1A and B, peak 4′) gave a single peak of disilylated migration. In addition, we have also performed GC-MS analysis of NC6 ceramide which gave again a single peak of disilylated form (data not shown).

A difficulty in the identification by GLC of ceramide molecular species in biological samples was the overlapping with diacylglycerols (26, 27). The mild-acid treatment was able to hydrolyze all diacylglycerols but also induced the partial hydrolysis of the amide bond of ceramide and sphingomyelin (50%, Fig. 1C). In addition, as indicated above, the acid treatment impairs the separation of sphingomyelin derivatives formed in the injection port and dehydrated ceramides. Thus, the mild-alkaline treatment was preferred, which cleaves ester bonds of glycerolipids but leaves unchanged ceramides, sphingomyelins, and glycosylceramides (34). Interestingly, the mild-alkaline treatment preserves mostly the esterified cholesterol molecular species (15% hydrolysis maximum was observed) (Fig. 3). Analysis of three different biological samples (plasma, HepG2, and CHO) was able to prove the efficiency of the method for a simultaneous analysis of molecular species of sphingomyelins, ceramides, and cholesteryl esters, all in the same injection. In plasma, the overall molecular species of sphingomyelins (525 nmol/ml) are in agreement with values previously reported (730 nmol/ml) (12), and display a similar profile for the major molecular species (C16:0-D18:1 and C24:1-D18:1) (27, 35). In addi-

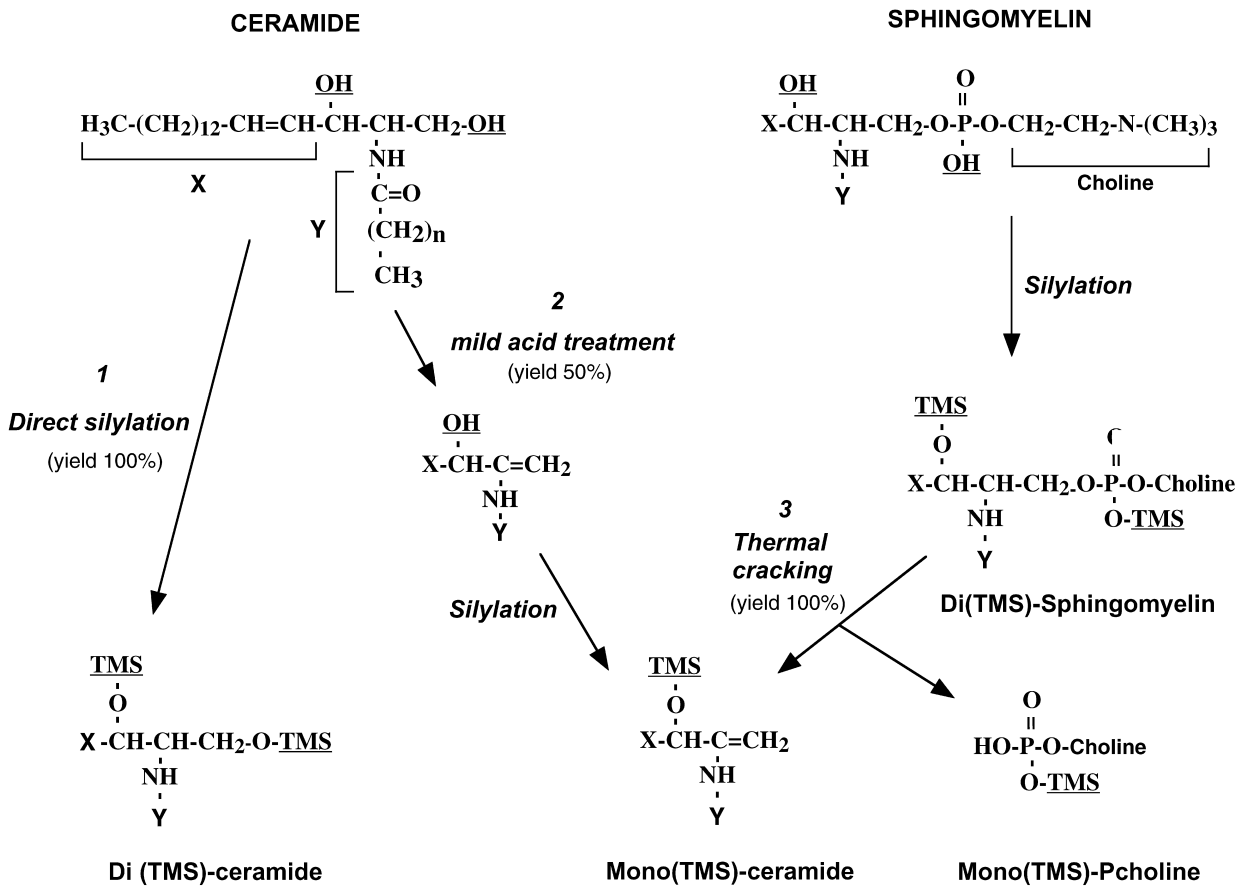

Fig. 9. A proposed mechanism of the formation of di- or mono-TMS ceramides from free ceramides or sphingomyelins. Direct silylation of free ceramide generates di-TMS ceramides (1); mild-acid treatment reaction of free ceramide (2) as well as thermal cracking of silylated sphingomyelins (3) generate mono-TMS ceramides.

tion, the fatty acid composition (Table 1) reflects that found in the different lipoprotein classes (13, 36, 37). In CHO and HepG2 cells, C16:0-D18:1 is also the major sphingomyelin molecular species as previously described for U937 cells (20). In contrast, C24:1-D18:1 is predominent in bovine brain (Fig. 1) (18). The method detects significant differences between CHO and HepG2 cells, (for instance, C16:0-D18:1 represents 54.9 vs. 12.3 nmol/mg protein, respectively), which also reflect the difference in the total sphingomyelin amounts (73.9 vs. 22.3 nmol/mg protein).

In human plasma, we did not detect any circulating ceramides at the detection limit of 5 pmol. In cultured cells, the quantitation of total ceramides corresponds to around 2 and 3 nmol/mg protein in CHO and HepG2 cells, respectively (Tables 2 and 3). These values are comparable with those obtained by other methods (HPLC, DG kinase assay, mass spectrometry) (5, 17, 20, 38, 39). A major advantage of the GLC technique is the straightforward determination of the ratio of ceramide to sphingomyelin within the same run. The ratio shows wide differences between cell lines (14.4% and 2.6% for HepG2 and CHO cells, respectively). The different molecular species are found similar to those found in HL60 cells (major C16:0-D18:1) (14), but different from skin fibroblats and U937 (17, 20).

When the metabolism of sphingomyelin/ceramide was studied in CHO cells upon treatment with a short chain permeant C6-ceramide, the sharp increase in the ceramide species C16:0-D18:1 correlated with the latter induction of apoptosis. The kinetics are in agreement with the appearance of C16:0-D18:1 (7-fold increase at 16 h) during apoptosis induced by ionizing radiation in Jurkat cells (40). The role of ceramide formation during the apoptotic process is questioned. For instance, addition of hexadecyl-phosphatidylcholine on HaCaT cells (39), ionizing radiation treatment of Jurkat (40), and PC12 cells under hypoxia (41), as well as TNFα and serum deprivation (5), equally induce apoptosis and the formation of ceramides. By contrast, Fas treatment of T-cells did not display any ceramide accumulation as measured by mass spectrometry (10). This points out the requirements for accurate methods to assay the low levels of cell ceramides as discussed in a recent review (21).

Apoptosis induction with short chain ceramide (20–50 μM) supports the view that ceramides are able to trigger apoptosis (42), but the inhibition of phospholipid biosynthesis, (43) as well as sphingomyelin and cholesterol alterations (44), has also been reported in this process. In our system, we observed the conversion of short chain ceramide to short chain sphingomyelin as described by others (44–47). In addition, our results support the hypothesis

that the large amounts of accumulating C16:0-D18:1, from 2 nmol in resting control cells to around 100 nmol/mg after 2 h of stimulation, reflect the conversion of the short chain C6 to the long chain C16 ceramide (44, 46). Indeed, although a slight increase was observed for NC16:0- and NC24:0-D18:1 SM at 2 h, as well as for NC24:0-D18:1 ceramide in the experiment (1.65-, 2.0- and 2.25-fold respectively), the 53.2-fold increase in the NC16:0-D18:1 ceramide already at 2 h, is in favor of a specific conversion/production of this molecular species. Whether the short chain sphingomyelin appearance represents a previous step to transacylation is a possibility that can be investigated with the method in the presence of inhibitor. It has also been proposed that the short chain ceramide effect was related to a competitive inhibition of the sphingomyelin synthesis in addition to the inhibition of the phosphatidylcholine biosynthesis (44).

The GLC method can provide an interesting insight into this mechanism by monitoring the sphingolipid-related cell products in the presence of various concentrations of the short chain ceramide. In conclusion, our method provides a new tool to study the variations in the molecular species of the major players of the sphingomyelin cycle during apoptosis.

The authors wish to thank Dr. Pierre Rogalle for helpful discussion concerning the synthesis of ceramides, and Dr. Klaebe for chemical analysis of ceramides.

Manuscript received 9 August 2001 and in revised form 15 November 2001.

REFERENCES

1. Hannun, Y. A., and R. M. Bell. 1989. Functions of sphingolipids and sphingolipids breakdown products in cellular regulation. *Science.* **243:** 500–507.
2. Kolesnick, R. N. 1991. Sphingomyelin and derivates as cellular signals. *Prog. Lipid Res.* **30:** 1–38.
3. Hannun, Y. A. 1994. The sphyngomyelin cycle and the second messager function of ceramides. *J. Biol. Chem.* **269:** 3125–3128.
4. Kolesnick, R. N., and M. Kronke. 1998. Regulation of ceramide production and apoptosis. *Annu. Rev. Physiol.* **60:** 643–665.
5. Hannun, Y. A. 1996. Functions of ceramide in coordinating cellular responses to stress. *Science.* **274:** 1855–1859.
6. Okazaki, T., R. M. Bell, and Y. A. Hannun. 1989. Sphingomyelin turnover induced by vitamin D3 in HL-60 cells. Role in cell differentiation. *J. Biol. Chem.* **264:** 19076–19080.
7. Tomiuk, S., K. Hofmann, M. Nix, M. Zumbansen, and W. Stoffel. 1998. Cloned mammalian neutral sphingomyelinase: functions in sphingolipid signaling? *Proc. Natl. Acad. Sci. USA.* **95:** 3638–3643.
8. Levade, T., N. Andrieu-Abadie, B. Segui, N. Auge, M. Chatelut, J. P. Jaffrezou, and R. Salvayre. 1999. Sphingomyelin-degrading pathways in human cells role in cell signalling. *Chem. Phys. Lipids.* **102:** 167–178.
9. Obeid, L. M., C. M. Linardic, L. A. Karolak, and Y. A. Hannun. 1993. Programmed cell death induced by ceramide. *Science.* **259:** 1769–1771.
10. Watts, J. D., M. Gu, A. J. Polverino, S. D. Patterson, and R. Aebersold. 1997. Fas-induced apoptosis of T cells occurs independently of ceramide generation. *Proc. Natl. Acad. Sci. USA.* **94:** 7292–7296.
11. Watts, J. D., M. Gu, S. D. Patterson, R. Aebersold, and A. J. Polverino. 1999. On the complexities of ceramide changes in cells undergoing apoptosis: lack of evidence for a second messenger function in apoptotic induction. *Cell Death Differ.* **6:** 105–114.
12. Kuksis, A., J. J. Myher, and K. Geher. 1993. Quantitation of plasma lipids by gas-liquid chromatography on high temperature polarizable capillary columns. *J. Lipid Res.* **34:** 1029–1038.
13. Myher, J. J., A. Kuksis, and S. Pind. 1989. Molecular species of glycerophospholipids and sphingomyelins of human plasma: comparison to red blood cells. *Lipids.* **24:** 408–418.
14. Fitzgerald, V., M. L. Blank, and F. Snyder. 1995. Molecular species of sphingomyelin in sphingomyelinase-sensitive and sphingomyelinase-resistant pools of HL-60 cells. *Lipids.* **30:** 805–809.
15. Merrill, A. H., E. Wang, R. E. Mullins, W. C. L. Jamison, S. Nimkar, and D. C. Liotta. 1988. Quantitation of free sphingosine in liver by high-performance liquid chromatography. *Anal. Biochem.* **171:** 373–381.
16. Morrison, W. R. 1969. Polar lipids in bovine milk. I. Long chain bases in sphingomyelin. *Biochim. Biophys. Acta.* **176:** 537–546.
17. Liebisch, G., W. Drobnik, M. Reil, B. Trumbach, R. Arnecke, B. Olgemoller, A. Roscher, and G. Schmitz. 1999. Quantitative measurement of different ceramide species from crude cellular extracts by electrospray ionization tandem mass spectrometry (ESI-MS/MS). *J. Lipid Res.* **40:** 1539–1546.
18. Kerwin, J. L., A. R. Tuininga, and L. H. Ericsson. 1994. Identification of molecular species of glycerophospholipids and sphingomyelin using electrospray mass spectrometry. *J. Lipid Res.* **35:** 1102–1114.
19. Bouh, J-F., and D. Bouh. 1984. Identification of free ceramide in human erythrocyte membrane. *J. Lipid Res.* **25:** 613–619.
20. Yano, M., E. Kishida, Y. Muneyuki, and Y. Masuzawa. 1998. Quantitative analysis of ceramide molecular species by high performance liquid chromatography. *J. Lipid Res.* **39:** 2091–2098.
21. Cremesti, A. E., and A. S. Fischl. 2000. Current methods for the identification and quantitation of ceramides: an overview. *Lipids.* **35:** 937–945.
22. Dijkman, R., N. Dekker, and G. H. de Haas. 1990. Competitive inhibition of lipolytic enzymes. II. Preparation of 'monoacylamino' phospholipids. *Biochim. Biophys. Acta.* **1043:** 67–74.
23. Bligh, E. G., and W. J. Dyer. 1959. A rapid method of total Lipid extraction and purification. *Can. J. Biochem. Physiol.* **37:** 911–917.
24. Lillington, J. M., D. J. H. Trafford, and H. L. J. Makin. 1981. A rapid and simple method for the esterification of fatty acids and steroid carboxylic acids prior to gas-liquid chromatography. *Clin. Chim. Acta.* **111:** 91–98.
25. Barrans, A., X. Collet, R. Barbaras, B. Jaspard, J. Manent, C. Vieu, H. Chap, and B. Perret. 1994. Hepatic lipase induces the formation of pre-beta 1 high density lipoprotein (HDL) from triacylglycerol-rich HDL2: a study comparing liver perfusion to in vitro incubation with lipases. *J. Biol. Chem.* **269:** 11572–11577.
26. Vieu, C., B. Jaspard, R. Barbaras, J. Manent, H. Chap, B. Perret, and X. Collet. 1996. Identification and quantification of diacylglycerols in HDL and accessibility to lipase. *J. Lipid Res.* **37:** 1153–1161.
27. Kuksis, A., and J. J. Myher. 1990. Gas-liquid chromatographic profiling of plasma lipid using high-temperature-polarizable capillary columns. *J. Chromatogr.* **500:** 427–441.
28. Barbaras, R., X. Collet, H. Chap, and B. Perret. 1994. Specific binding of free apolipoprotein A-I to a high-affinity binding site on HepG2 cells: characterization of two high-density lipoprotein sites. *Biochemistry.* **33:** 2335–2340.
29. Cui, Z., M. Houweling, M. H. Chen, M. Record, H. Chap, D. E. Vance, and F. Terce. 1996. A genetic defect in phosphatidylcholine biosynthesis triggers apoptosis in Chinese hamster ovary cells. *J. Biol. Chem.* **271:** 14668–14671.
30. Lowry, O. H., N. J. Rosebrough, A. L. Farr, and R. J. Randall. 1951. Protein measurement with the folin phenol reagent. *J. Biol. Chem.* **193:** 265–275.
31. Roschlau, P., E. Bernet, and N. Gruber. 1974. Enzymatische bestimmung des gesamtcholesterins im serum. *Z. Klin. Chem. Klin. Biochem.* **12:** 403–407.
32. Böttcher, C. J. F., C. M. Van Gent, and C. Pries. 1961. A rapid sensitive submicrophosphorus determination. *Anal. Chim. Acta.* **24:** 203–204.
33. Joo, F., F. Chevy, O. Colard, and C. Wolf. 1993. The activation of rat platelets increases the exposure of polyunsaturated fatty acid enriched phospholipids on the external leaflet of the plasma membrane. *Biochim. Biophys. Acta.* **1149:** 231–240.
34. Vance, D. E., and C. C. Sweeley. 1967. Quantitative determination of the neutral glycosyl ceramides in human blood. *J. Lipid Res.* **8:** 621–630.
35. Samuelsson, B., and L. Samuelsson. 1969. Separation and identifi-

cation of ceramides derived from human plasma sphingomyelins. *J. Lipid Res.* **10:** 47–55.
36. Myher, J. J., A. Kuksis, W. C. Breckenridge, and J. A. Little. 1981. Differential distribution of sphingomyelins among plasma lipoprotein classes. *Can. J. Biochem.* **59:** 626–636.
37. Katsikas, H., and C. Wolf. 1995. Blood sphingomyelins from two European countries. *Biochim. Biophys. Acta.* **1258:** 95–100.
38. Krivit, W., and S. Hammarström. 1972. Identification and quantitation of free ceramides in human platelets. *J. Lipid Res.* **13:** 525–530.
39. Wieder, T., C. E. Orfanos, and C. C. Geilen. 1998. Induction of ceramide-mediated apoptosis by the anticancer phospholipid analog, hexadecylphosphocholine. *J. Biol. Chem.* **273:** 11025–11031.
40. Thomas, R. L., C. M. Matsko, M. T. Lotze, and A. A. Amoscato. 1999. Mass spectrometric identification of increased C16 ceramide levels during apoptosis. *J. Biol. Chem.* **274:** 30580–30588.
41. Yoshimura, S., Y. Banno, S. Nakashima, K. Takenaka, H. Sakai, Y. Nishimura, N. Sakai, S. Shimizu, Y. Eguchi, Y. Tsujimoto, and Y. Nozawa. 1998. Ceramide formation leads to caspase-3 activation during hypoxic PC12 cell death: inhibitory effects of Bcl-2 on ceramide formation and caspase-3 activation. *J. Biol. Chem.* **273:** 6921–6927.
42. Zhou, H., S. A. Summers, M. J. Birnbaum, and R. N. Pittman. 1998. Inhibition of Akt kinase by cell-permeable ceramide and its implications for ceramide-induced apoptosis. *J. Biol. Chem.* **273:** 16568–16575.
43. Bladergroen, B. A., M. Bussiere, W. Klein, M. J. Geelen, L. M. Van Golde, and M. Houweling. 1999. Inhibition of phosphatidylcholine and phosphatidylethanolamine biosynthesis in rat-2 fibroblasts by cell-permeable ceramides. *Eur. J. Biochem.* **264:** 152–160.
44. Allan, D. 2000. Lipid metabolic changes caused by short-chain ceramides and the connection with apoptosis. *Biochem. J.* **345:** 603–610.
45. Pagano, R. E., O. C. Martin, H. C. Kang, and R. P. Haugland. 1991. A novel fluorescent ceramide analogue for studying membrane traffic in animal cells: accumulation at the Golgi apparatus results in altered spectral properties of the sphingolipid precursor. *J. Cell Biol.* **113:** 1267–1279.
46. Ridgway, N. D., and D. L. Merriam. 1995. Metabolism of short-chain ceramide and dihydroceramide analogues in Chinese hamster ovary (CHO) cells. *Biochim. Biophys. Acta.* **1256:** 57–70.
47. Fukasawa, M., M. Nishijima, and K. Hanada. 1999. Genetic evidence for ATP-dependent endoplasmic reticulum-to-Golgi apparatus trafficking of ceramide for sphingomyelin synthesis in Chinese hamster ovary cells. *J. Cell Biol.* **144:** 673–685.